Inhibition of Metastatic Outgrowth from Single Dormant Tumor Cells by Targeting the Cytoskeleton

Dalit Barkan,[1] Hynda Kleinman,[2] Justin L. Simmons,[1] Holly Asmussen,[1] Anil K. Kamaraju,[1] Mark J. Hoenorhoff,[1] Zi-yao Liu,[1] Sylvain V. Costes,[4] Edward H. Cho,[5] Stephen Lockett,[5] Chand Khanna,[3] Ann F. Chambers,[6] and Jeffrey E. Green[1]

[1]Laboratory of Cell Biology and Genetics, National Cancer Institute, [2]Craniofacial Developmental Biology and Regeneration Branch, National Institute of Dental and Craniofacial Research, and [3]Pediatric Oncology Branch, National Cancer Institute, NIH, Bethesda, Maryland; [4]Cancer Biology Department, Lawrence Berkeley National Laboratory, Berkeley, California; [5]Image Analysis Laboratory, Science Applications International Corporation-Frederick, National Cancer Institute at Fredrick, Fredrick, Maryland; and [6]London Regional Cancer Program, London, Ontario, Canada

Abstract

Metastatic breast cancer may emerge from latent tumor cells that remain dormant at disseminated sites for many years. Identifying mechanisms regulating the switch from dormancy to proliferative metastatic growth has been elusive due to the lack of experimental models of tumor cell dormancy. We characterized the *in vitro* growth characteristics of cells that exhibit either dormant (D2.0R, MCF-7, and K7M2AS1.46) or proliferative (D2A1, MDA-MB-231, and K7M2) metastatic behavior *in vivo*. Although these cells proliferate readily in two-dimensional culture, we show that when grown in three-dimensional matrix, distinct growth properties of the cells were revealed that correlate to their dormant or proliferative behavior at metastatic sites *in vivo*. In three-dimensional culture, cells with dormant behavior *in vivo* remained cell cycle arrested with elevated nuclear expression of p16 and p27. The transition from quiescence to proliferation of D2A1 cells was dependent on fibronectin production and signaling through integrin β1, leading to cytoskeletal reorganization with filamentous actin (F-actin) stress fiber formation. We show that phosphorylation of myosin light chain (MLC) by MLC kinase (MLCK) through integrin β1 is required for actin stress fiber formation and proliferative growth. Inhibition of integrin β1 or MLCK prevents transition from a quiescent to proliferative state *in vitro*. Inhibition of MLCK significantly reduces metastatic outgrowth *in vivo*. These studies show that the switch from dormancy to metastatic growth may be regulated, in part, through epigenetic signaling from the microenvironment, leading to changes in the cytoskeletal architecture of dormant cells. Targeting this process may provide therapeutic strategies for inhibition of the dormant-to-proliferative metastatic switch. [Cancer Res 2008;68(15):6241–50]

Introduction

Recurrence of breast cancer often follows a long latent period where metastases may become clinically apparent many years after removal of the primary tumor and adjuvant therapy. Recent evidence suggests that in many such cases, tumor cells have already seeded metastatic sites, although the primary disease is diagnosed at an early stage (1–3). Approximately 30% and 74% of breast cancer patients diagnosed at the M0 or M1 tumor-node-metastasis tumor stages, respectively, were found to have breast cancer cells in their bone marrow, although these cells seem to primarily exist as micrometastases that are not clinically manifested (1). Most of these micrometastatic cells do not express proliferation markers and, therefore, represent quiescent dormant tumor cells (QTC), also referred to as cellular dormancy (1, 4–6). These cells are resistant to conventional therapies that target actively dividing cells (1, 7), which likely accounts for disease recurrence following apparent successful treatment of primary tumors. It has been proposed that cellular dormancy represents an early, quiescent phase of tumor cell dormancy that may progress to proliferative micrometastases, whose size is limited by the lack of an angiogenic response, which may ultimately transit through an angiogenic switch and become clinically apparent metastases (6, 8).

Dissecting the mechanisms that either maintain prolonged cellular dormancy or activate dormant tumor cells to proliferate and developing therapeutic approaches to eliminate dormant tumor cells have been hampered by the lack of model systems that mimic the *in vivo* behavior of cellular dormancy and the emergence of clinical metastatic disease. Traditional two-dimensional cell culture techniques fail to recapitulate the *in vivo* dormant behavior of tumor cells. For instance, our previous work showed that D2.0R mammary tumor cells exhibit dormant behavior at metastatic sites when injected into mice, but these cells readily proliferate when cultured in two-dimensional conditions (5), suggesting that the microenvironment may play an important role in tumor cell dormancy.

The tumor microenvironment has been increasingly recognized as a critical regulator of cancer progression (reviewed in refs. 6, 9, 10). The extracellular matrix (ECM), a key component of the microenvironment, is in immediate contact with the tumor cells and functions as a critical source for growth, survival, motility, and angiogenic factors that significantly affect tumor biology and progression. Additionally, cell adhesion to the ECM triggers intracellular signaling pathways that can regulate cell cycle progression, migration, and differentiation (11, 12) through integrins and other cell surface receptors. Thus, interactions between tumor cells and the ECM are critical modulators of the metastatic potential of tumor cells.

Culturing cells in three-dimensional basement membrane cultures has been used in the past to study morphogenesis, differentiation, tumorigenesis, motility, and invasion of cells through the basement membrane (12, 13). In this study, we

Note: Supplementary data for this article are available at Cancer Research Online (http://cancerres.aacrjournals.org/).

Requests for reprints: Jeffrey E. Green, Laboratory of Cell Biology and Genetics, National Cancer Institute, NIH, Building 37, Room 4054, 37 Convent Drive, Bethesda, MD 20892. Phone: 301-435-5193; Fax: 301-496-8709; E-mail: jegreen@nih.gov.

doi:10.1158/0008-5472.CAN-07-6849

characterize a novel three-dimensional *in vitro* system in which growth characteristics of several tumor cell lines in ECM correlate with the dormant or proliferative behavior of the tumor cells at a metastatic secondary site *in vivo*. Our results reveal that a stage of prolonged tumor cell quiescence, presumably preceding a later stage that is dependent on angiogenesis for metastatic growth, exists due to cell cycle arrest. However, we show that the switch from quiescence to proliferative metastatic growth is strongly influenced by interactions with the ECM. Specifically, we show that fibronectin signaling through integrin β1 induces the switch from quiescence to proliferative growth. The transition is associated with dramatic reorganization of the cytoskeleton and activation of myosin light chain kinase (MLCK). Pharmacologic and short hairpin RNA (shRNA) targeting of cytoskeletal reorganization via inhibition of MLCK inhibited metastatic growth of QTCs *in vivo*, suggesting that interference with cytoskeletal reorganization may be an important avenue for preventing recurrent disseminated disease.

Materials and Methods

Three-dimensional cell cultures. Mouse mammary cancer cells D2.0R, D2A1 (5, 14), and 4T1 (obtained from Dr. Fred Miller, Barbara Ann Karmanos Cancer Institute, Detroit, MI; ref. 15), mouse osteosarcomas K7M2 and K7M2AS1.46 cells (16), human MDA-MB-231 [American Type Culture Collection (ATCC)], MDA-MB-231 stably expressing green fluorescent protein (GFP; obtained from Dr. Danny Welch, University of Alabama at Birmingham, Birmingham, AL; ref. 17), and MCF-7 breast cancer cells (ATCC) were maintained in DMEM high glucose, 10% fetal bovine serum (FBS), and antibiotics (Life Technologies). The cells were cultured in growth factor–reduced three-dimensional Cultrex Basement Membrane Extract (Trevigen, Inc.), as previously described (18), with slight modifications as described in Supplementary Materials and Methods. Cell morphology was monitored by light microscopy, and time-lapse images were captured by a Zeiss LSM 510 confocal laser scanning microscope. ML-7 (Biomol International L.P.) and W13 (Calbiochem) were used to inhibit MLCK and calmodulin, respectively. Antibody against integrin β1 clone 9EG7 sodium azide–free was used to neutralize integrin β1 function (BD Biosciences) and control cultures were treated with the same concentration of nonspecific IgG.

shRNA silencing experiments. A shRNA expression vector targeting MLCK was generated as described in Supplementary Materials and Methods. Scrambled shRNA was used as a negative control. shRNA was transfected to D2A1 cells (0.5×10^6) using Amaxa Nucleofector technology (Amaxa, Inc.), trypsinized (Invitrogen) after 48 h, and cultured in three dimensional for 5 d. In parallel, RNA was isolated from the transfected cells from two-dimensional culture at 120 h. The RNA was reverse transcribed using RNase H^- reverse transcriptase (SuperScript II, Invitrogen). Semiquantitative PCR was repeated in triplicate using the following MLCK primers: 5′-CTCGGAACCTCTGCGTCAAAG-3′ (forward) and 5′-CAGTCTACCATGTCAACGCTA-3′ (reverse).

Proliferation assay. Ninety-six–well plates were coated with 50 to 100 μL Cultrex. Cells were resuspended in 100 μL DMEM low glucose supplemented with 2% FBS and 2% Cultrex or 2% FBS supplemented with Cultrex + fibronectin and grown on the coated plates. Cells (1.5×10^3 to 2×10^3 per well) for D2A1, D2.0R, MDA-MB-231, MCF-7, and 4T1 and 2.0×10^3 cells per well for K7M2 and K7M2AS1.46. The CellTiter 96 AQueous One Solution cell proliferation assay kit (Promega) was used to measure cell proliferation as described in Supplementary Materials and Methods.

Immunostaining. Cells (1×10^4) were cultured in three-dimensional Cultrex using 24-well plates coated with 300 μL Cultrex. The cells were fixed with 10% buffered formalin. Paraffin sections were analyzed by H&E, terminal deoxynucleotidyl transferase–mediated dUTP nick end labeling (TUNEL) staining, and Ki67 (Vector Laboratories) immunohistochemistry. Immunostaining for p27 (1:50; Medical and Biological Laboratories) and p16 (1:50; Santa Cruz Biotechnology) was carried out with the DAKO ARK Peroxidase kit (DAKO). Antigen retrieval was carried out for p27 staining using citrate buffer. Multiple sections from the three-dimensional Cultrex blocks were analyzed. At least 100 cells were analyzed for immunoreactivity.

Animal studies. D2A1 and MCF cells were infected with the lentivirus pHR-GFP and D2.0R cells were infected with pSico-GFP (19). MCF-7, MDA-MB-231, and D2A1 stably expressing GFP were additionally labeled with CellTracker Green 5-chloromethylfluorescein diacetate according to the manufacturer's protocol (Molecular Probes). Four- to 6-wk-old female BALB/c-*nu/nu* athymic mice were injected via tail vein with 1×10^6 cells. In the case of MCF-7 cells, the mice were implanted 24 h after injection with 0.36 mg/pellet 17β-estradiol for 60 d. Cytoskeletal organization and immunostaining were examined in dormant and proliferating metastatic cells *in vivo* as described in Supplementary Materials and Methods. For inhibition of MLCK activity in D2A1 cells *in vivo*, mice were injected with D2A1 cells stably expressing GFP and labeled with CellTracker. Mice were anesthetized 24 h after injection and a small horizontal incision was made in the interscapular area into which a 200 μL osmotic pump (Alzet) with a 0.25 μL/h release rate was implanted containing either ML-7 (22 mmol/L) in DMSO (experimental group) or DMSO (control group). Mice were sacrificed after 1 wk, and lungs were removed, inflated with PBS, and subjected to single-cell whole organ microscopy (SCOM) imaging immediately. All mice were treated in accordance with the guidelines of the Animal Care and Use of Laboratory Animals (NIH Publication No. 86-23, 1985) under an approved animal protocol.

***In vivo/ex vivo* imaging.** Lungs removed from the mice, as described in Supplementary Materials and Methods, were imaged by inverted fluorescent videomicroscopy (Leica DM IRB) at ×25 and ×100 magnification. The whole lung was sequentially captured for each mouse at ×100 magnification. Each captured frame was analyzed using OpenLab software to measure the surface area of the metastases that are larger than 10 pixels. The percentage of lesions <1,000 pixels (single cells) versus lesions >1,000 pixels.

Immunofluorescence. Staining for filamentous actin (F-actin), integrin β1, and fibronectin *in vitro* was carried out by overnight incubation, as described in Supplementary Materials and Methods. Frozen lung sections (8 μm) were fixed with 4% paraformaldehyde for 10 min, washed with PBS (thrice for 5 min), and blocked with 5% bovine serum albumin (Sigma) for 15 min. Slides were then washed thrice with PBS (as above) and incubated with Alexa Texas Red-X phalloidin (1:20; Molecular Probes) for 1 h at 37°C, washed thrice with PBS, and mounted with Vectashield mounting medium with 4′,6-diamidino-2-phenylindole (DAPI). The slides were imaged using a Leica confocal microscope (Leica Microsystems AG).

Statistical analyses. Student's *t* test was used for the proliferation assays and for the *in vivo* analysis. Statistical significance was defined as $P \leq 0.05$ (*), $P \leq 0.001$ (**), and $P \leq 0.0001$ (***).

Results

***In vitro* model for solitary tumor cell dormancy.** To explore whether the ECM influences the dormant (nonproliferative) or proliferative behavior of metastatic cells, we initially studied the well-characterized D2.0R and related D2A1 mammary tumor cell model system for tumor cell dormancy (5, 7, 20). When injected into mice, D2.0R cells invade distant metastatic sites, remain as single quiescent cells for prolonged periods of time, but occasionally may emerge from a dormant state and proliferate into metastatic tumors. In contrast, D2A1 cells remain dormant for a relatively short period of time following injection and subsequently form numerous metastatic tumors quite rapidly compared with D2.0R cells. Despite the divergent behavior of these cells *in vivo*, both cell lines readily proliferate when cultured in two dimensional on a plastic substrate (Fig. 1*A*). When these cells are cultured in three-dimensional Cultrex basement membrane extracted from a transplantable murine tumor, D2.0R cells

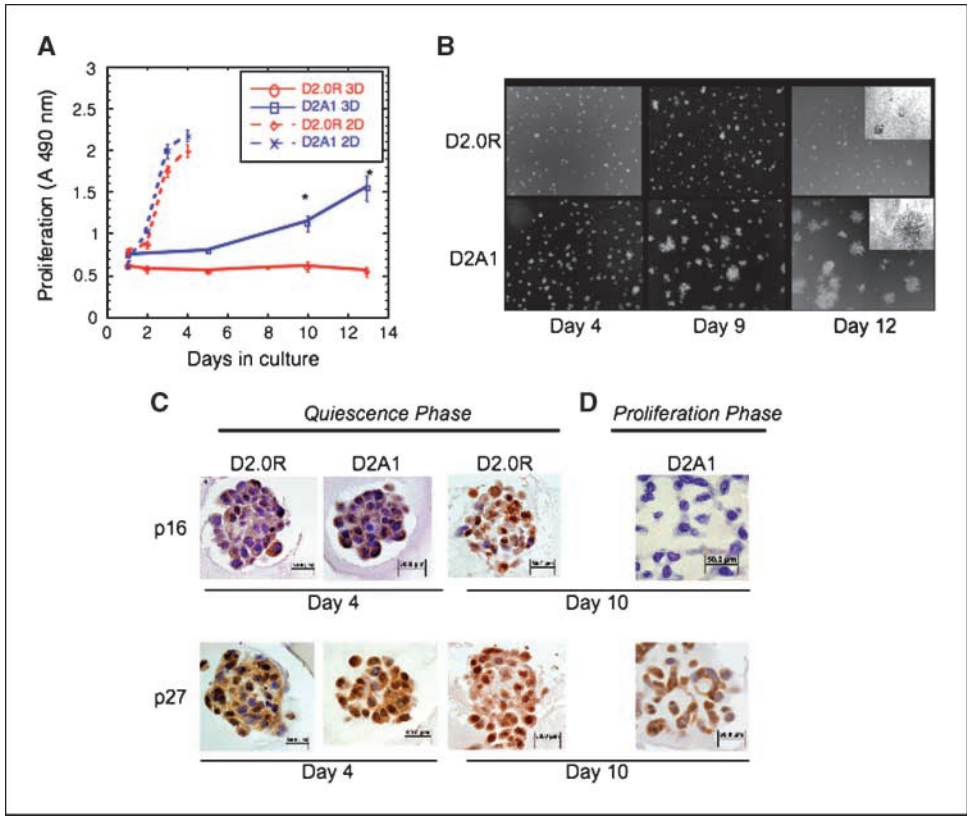

Figure 1. *In vitro* model for solitary tumor cell dormancy. *A,* proliferation of D2.0R and D2A1 in two-dimensional culture and in three-dimensional Cultrex (as described in Materials and Methods). *Points,* mean ($n = 8$); *bars,* SE. Representative result of three experiments. *, $P \leq 0.05$. *B,* D2.0R and D2A1 cells were cultured in three-dimensional Cultrex (as described in Materials and Methods). Images of the cells were acquired at days 4, 9, and 12. Magnification, ×20. *Top right,* magnification, ×40. *C* and *D,* quiescence in the three dimensional culture is associated with elevated p16 and p27. Immunohistochemical staining for p16 and p27. *C,* quiescent phase: D2.0R cells, culture days 4 and 10; D2A1 cells, day 4. *D,* proliferative phase of D2A1 cells, day 10. Note loss of p16 expression and reduction of p27 nuclear localization during D2A1 proliferative phase, but continued high expression in quiescent D2.0R cells. Magnification, ×40.

do not proliferate but remain quiescent through the entire experimental 14-day culture period (Fig. 1*A* and *B*), whereas the highly metastatic D2A1 cells only remain quiescent for 4 to 6 days after which they begin to proliferate (Fig. 1*A* and *B*). During the initial quiescent phase of both cell lines in the three-dimensional culture, many cells remain solitary, whereas other nonproliferating cells aggregate and form multicellular spheroids (Supplementary Fig. S1; Supplementary Videos 1 and 2). Thus, these initial studies suggested that when exposed to a three-dimensional environment *in vitro*, the distinct growth characteristics of these cells could be correlated to their dormant or proliferative behavior at the metastatic sites *in vivo*.

Solitary dormant tumor cells are cell cycle arrested. To determine the growth dynamics of D2.0R and D2A1 cells in three-dimensional culture, staining for the proliferation marker Ki67 and for apoptosis (TUNEL assay) was performed at day 4 of *in vitro* culture when no differences in overall cell number were observed for both cell lines. Few D2.0R or D2A1 cells exhibited nuclear staining for Ki67 (5% and 7%, respectively), and TUNEL staining for apoptosis was negative in both cell lines (data not shown). D2.0R and D2A1 cells exhibited low levels of nuclear staining for p16 at culture day 4 (13% and 17%, respectively; Fig. 1*C*). However, in both cell lines, >60% of the nuclei stained positively for p27 (Fig. 1*C*). After 10 days in culture, only 25% of D2A1 cells exhibited nuclear staining for p27 (Fig. 1*D*). Similarly, p16 staining was absent in proliferating D2A1 cells at day 10 (Fig. 1*D*), whereas 50% of the nuclei of D2.0R cells stained positively for p16 and 77% of the nuclei stained positively for p27 at day 10 (Fig. 1*C*). Thus, the lack of growth of these cell types in three-dimensional culture is not a consequence of a balance between apoptosis and proliferation but rather due to cell cycle arrest.

Three-dimensional culture as a predictive model for cellular dormancy. The growth characteristics of additional cell lines with known *in vivo* metastatic growth properties were assessed. The metastatic mammary cancer cell lines, human MDA-MB-231 and mouse 4T1 cells, and the human MCF-7 cell line, which rarely develops metastases when injected into nude mice (21), were investigated using the three-dimensional system. MDA-MB-231 cells remained quiescent for only 2 days in three-dimensional culture and subsequently began to proliferate at day 3, whereas 4T1 cells proliferated within 1 day in three-dimensional culture (Fig. 2*A* and *B*). In contrast, MCF-7 cells remained quiescent for the 14-day culture period (Fig. 2*A* and *B*). Similar to D2.0R cells, a high percentage (50%) of MCF-7 cells showed nuclear staining for p27 at day 10 (data not shown).

Importantly, we determined that MCF-7 cells exhibit dormant properties when disseminated to the lung as a metastatic site. GFP-expressing MCF-7 and MDA-MB-231 cells were injected via tail vein into nude mice (see Materials and Methods). Lungs were removed 2 weeks after tail vein injection for GFP-expressing MDA-MB-231 cells (due to the rapid development of metastases) or 9 weeks after injection for MCF-7-GFP–expressing cells (which had not developed multicellular metastases by that time) and imaged using fluorescent single cell whole organ microscopy (SCOM; ref. 16) and analyzed histologically. Whereas MDA-MB-231 cells developed large metastases (Fig. 2*C*), only scattered individual MCF-7 cells were found in the lungs with no evidence of proliferating, multicellular metastases (Fig. 2*C*). Isolated MCF-7 cells were similarly identified in mice 6 months after cell injection (data not shown). Thus, the growth characteristics of MDA-MB-231 and MCF-7 cells in three-dimensional culture correlated with their dormant or poor metastatic growth potential *in vivo*.

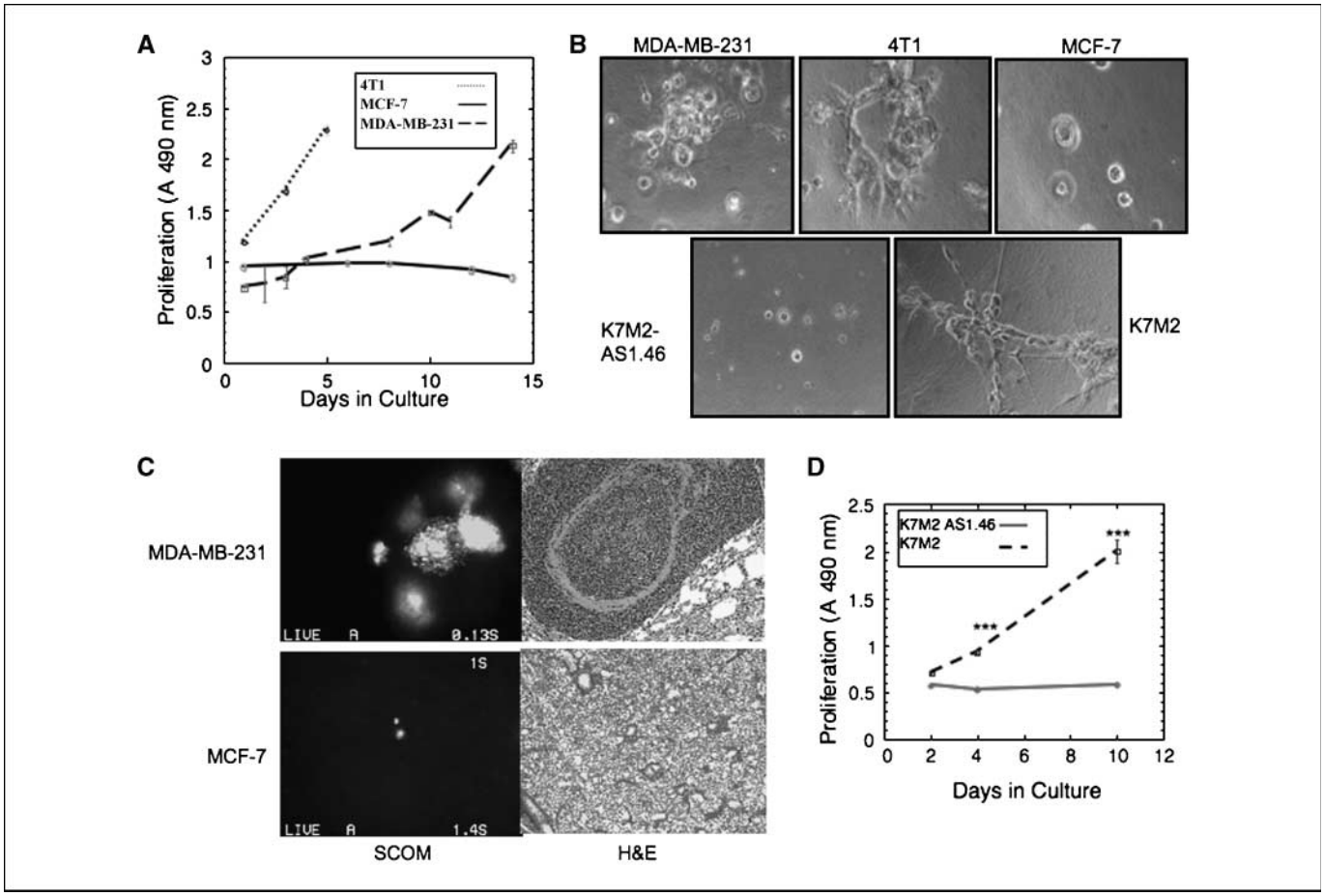

Figure 2. Correlation of *in vivo* dormant or metastatic behavior of tumor cells with growth in three-dimensional culture. *A,* proliferation of MDA-MB-231, 4T1, and MCF-7 cells in three-dimensional Cultrex. *Points,* mean ($n = 8$); *bars,* SE. Representative result of three experiments. *B,* morphology of MDA-MB-231, 4T1, MCF-7, K7M2AS1.46, and K7M2 cells cultured in three-dimensional Cultrex. Magnification, ×40. *C,* representative lungs from a mouse injected with GFP-expressing MDA-MB-231 (2 wk after injection) or MCF-7 cells (9 wk after injection). *Left,* SCOM images of MDA-MB-231 lung metastasis and dormant MCF-7 cell. Magnification, ×100. *Right,* representative H&E staining of MDA-MB-231 lung metastasis and of lung with MCF-7 cells lacking proliferative metastases. Magnification, ×20. *D,* proliferation of K7M2 and K7M2AS1.46 cells in three-dimensional Cultrex. *Points,* mean ($n = 8$); *bars,* SE. Representative result of three experiments. ***, $P \leq 0.001$.

Similar results were obtained for the previously described mouse osteosarcoma cell lines K7M2 (highly metastatic) and K7M2AS1.46, a clonal derivative of K7M2 engineered to express reduced levels of ezrin. Unlike K7M2 cells, which are highly metastatic, the K7M2AS1.46 cells seed metastatic sites when injected *in vivo* but do not form pulmonary metastases (16). Although both cell lines proliferate similarly in two-dimensional culture (data not shown), when introduced into the three-dimensional culture system, K7M2AS1.46 cells remain quiescent through the 14-day experimental period, whereas K7M2 cells were quiescent for only 4 days and subsequently began to proliferate (Fig. 2*B* and *D*).

Interaction with the ECM alters cytoskeletal architecture and influences the dormant-to-proliferative switch. The transition of D2A1 cells from a quiescent to proliferative state in three-dimensional culture (Fig. 1*B*) was associated with dramatic changes in cell morphology. Therefore, we examined changes in cytoskeleton reorganization during the transition from quiescence to proliferation.

Both D2.0R and D2A1 cells formed filopodia during their quiescent phase in three-dimensional culture (Supplementary Fig. S2*A* and *B*). Cells were stained with phalloidin on days 1, 4, and 7 to observe the organization of F-actin fibers (Fig. 3*A*). D2.0R cells displayed cortical F-actin staining at all time points (Fig. 3*A, arrowheads*). In contrast, F-actin stress fibers began to appear in D2A1 cells on day 4 (before cell proliferation, as seen in Fig. 1*B, arrow*) and were most prominent in proliferating cells on day 7 (Fig. 3*A, arrows*). Increased phosphorylation of MLC, which is required for actin stress fiber formation (22), was elevated in D2A1 cells at days 4 and 7, correlating with extensive actin stress fiber formation (Fig. 3*B, arrows*; Supplementary Fig. S2*C*) and the transition from a quiescent to a proliferative state. Similarly, the metastatic 4T1, MDA-MB-231, and K7M2 cells formed actin stress fibers in the three-dimensional *in vitro* system in association with proliferation (Fig. 3*C, arrows*). Like D2.0R cells, nonmetastatic MCF-7 and K7M2AS1.46 cells displayed only cortical F-actin staining (Fig. 3*C, arrowheads*). Thus, all of the nonproliferating cells studied exhibited only cortical F-actin localization, whereas cells that were emerging from quiescence had extensive stress fiber formation.

Similar cytoskeletal reorganization was observed *in vivo*. Lungs removed from nude mice tail vein injected with GFP-expressing D2A1, D2.0R, MCF-7, or MDA-MB-231 cells (1×10^6 per mice) were imaged by SCOM (Fig. 4*A*), and sections were then stained for F-actin (Fig. 4*B*). Single dormant D2A1-GFP cells were apparent at

1 and 7 days after injection (Fig. 4*A*) and exhibited cortical staining for F-actin (Fig. 4*B, arrowheads*). However, D2A1-GFP cells in growing metastatic lesions 3 weeks after injection (Fig. 4*A*) displayed cytoskeletal reorganization and formation of actin stress fibers (Fig. 4*B, arrows*). Solitary dormant D2.0R-GFP cells (Fig. 4*A*) with cortical F-actin staining (*arrowheads*) were detected 4 weeks after injection, whereas one of five injected mice developed metastasis after 12 weeks (Fig. 4*A*) that exhibited actin stress fiber formation (Fig. 4*B, arrows*). Similarly, metastatic lesions from the MDA-MB-231 cell line (Fig. 4*A*) formed actin stress fibers (Fig. 4*B, arrows*), whereas solitary dormant MCF-7 cells (Fig. 4*A*) displayed only cortical F-actin staining (Fig. 4*B, arrowheads*). These results show that actin stress fiber formation is associated with proliferative metastatic growth *in vivo*.

MLCK activation is required for actin stress fiber formation and the transition from dormancy to growth. To determine whether formation of actin stress fibers is required for the transition from a quiescence to proliferation, phosphorylation of MLC by MLCK, required for F-actin stress fiber formation, was inhibited by (*a*) ML-7, a specific inhibitor of MLCK (23); (*b*) shRNA to target MLCK RNA; or (*c*) W13, a specific inhibitor of Ca^{2+} calmodulin that regulates MLCK activity (24). MLCK expression was significantly reduced by transfection of a MLCK shRNA-expressing vector (see Supplementary Fig. S3*A*). MLCK activity in D2A1 cells was inhibited at day 5 with either ML-7, W13, or transfection of the MLCK shRNA-targeting vector, leading to a reduction in phosphorylated MLC (localized mainly to the cytoplasmic membrane), disruption of actin stress fibers, and the rounding of cells (Fig. 5*A*). Cell proliferation was reduced ($P \leq 0.05$; Fig. 5*B*) and p27 nuclear staining increased from 30% positive nuclei in the nontreated cells to 50% positive nuclei in ML-7–treated cells (Supplementary Fig. S3*B, arrow*). ML-7 also significantly inhibited proliferation ($P \leq 0.05$) in MDA-MB-231 and 4T1 cells (Supplementary Fig. S3*C*). These results show that MLCK activity and the formation of actin stress fibers are required for the transition of these metastatic cells from a quiescent to a proliferative state *in vitro*.

The role of MLCK was further assessed *in vivo*. Nude mice were tail vein injected with D2A1-GFP cells also labeled with CellTracker and treated systemically with either ML-7 or vehicle. *In vivo* targeted effects of ML-7 inhibition of MLC phosphorylation were shown (see Supplementary Fig. S3*D*). Lungs were removed, tumor cells were imaged by SCOM, and the areas of lung metastases were quantified by fluorescent signal. The vast majority (80%) of the metastatic lesions present in ML-7–treated mice persisted as single cells displaying cortical F-actin organization (data not shown), whereas in the untreated control mice only 30% of the lesions were single cells and 70% of the metastatic lesions were clusters of cells ($P \leq 0.001$; Fig. 5*C*). Thus, inhibition of MLCK by ML-7 can significantly reduce the progression of solitary dormant tumor cells to proliferating metastatic lesions.

Fibronectin activation of MLCK through integrin β1 signaling activates the transition from quiescence to growth. Because fibronectin has been identified as one of several ECM genes in gene expression signatures related to breast cancer metastases (25, 26), we explored whether this ECM protein might play a role in the dormant-to-proliferative switch in the three-dimensional system because Cultrex does not contain fibronectin.

D2A1 cells express very low levels of fibronectin by day 5 in three-dimensional culture (data not shown), which significantly increases by day 7 (Fig. 6*A*). Similarly, lung lesions of D2A1-GFP cells express fibronectin (Supplementary Fig. S4*A*). In contrast,

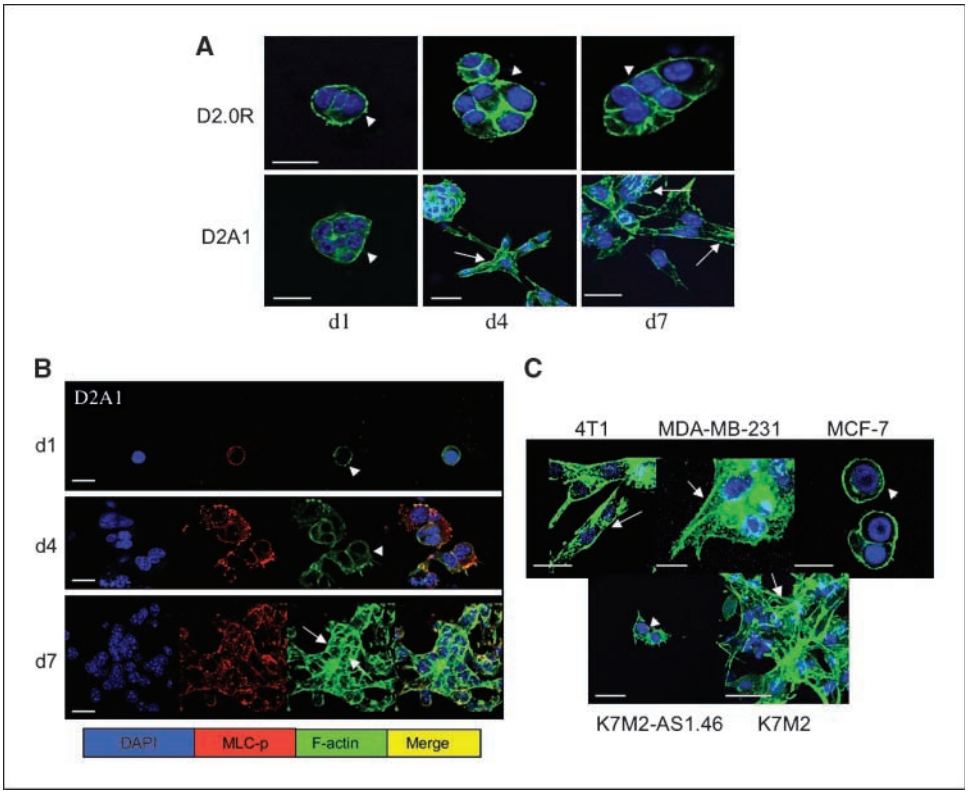

Figure 3. Actin stress fiber formation associated with MLC phosphorylation occurs during the transition from quiescence to growth in three-dimensional culture. D2.0R, D2A1, MCF-7, MDA-MB-231, 4T1, K7M2, and K7M2AS1.46 cells were cultured in three-dimensional Cultrex on glass coverslips (as described in Materials and Methods). Cells were fixed and stained with DAPI (*blue*) for nuclear localization, phalloidin (*green*) for F-actin, and an antibody against the phosphorylated form of MLC (*red*), as indicated at various time points, using confocal microscopy (magnification, ×63). *A,* proliferative growth is associated with actin stress fiber formation. *Arrowheads,* cortical F-actin staining was evident in D2.0R cells at day 1 (*d1*), day 4 (*d4*), and day 7 (*d7*). D2A1 cells exhibited cortical F-actin at day 1 (*arrowhead*), but actin stress fibers form at days 4 and 7 (*arrows*). *B,* actin stress fiber formation and proliferative growth is associated with MLC phosphorylation. D2A1 cells show localization of phosphorylated MLC with actin at day 1 (*d1*) and with actin stress fibers by day 7 (*d7*). *C,* 4T1 and MDA-MB-231 (day 4) and K7M2 cells (day 6) displayed actin stress fibers (*arrows*), whereas nonproliferative MCF-7 (day 14) and K7M2AS1.46 (day 10) displayed cortical F-actin staining (*arrowheads*). *Scale bars,* 20 μm.

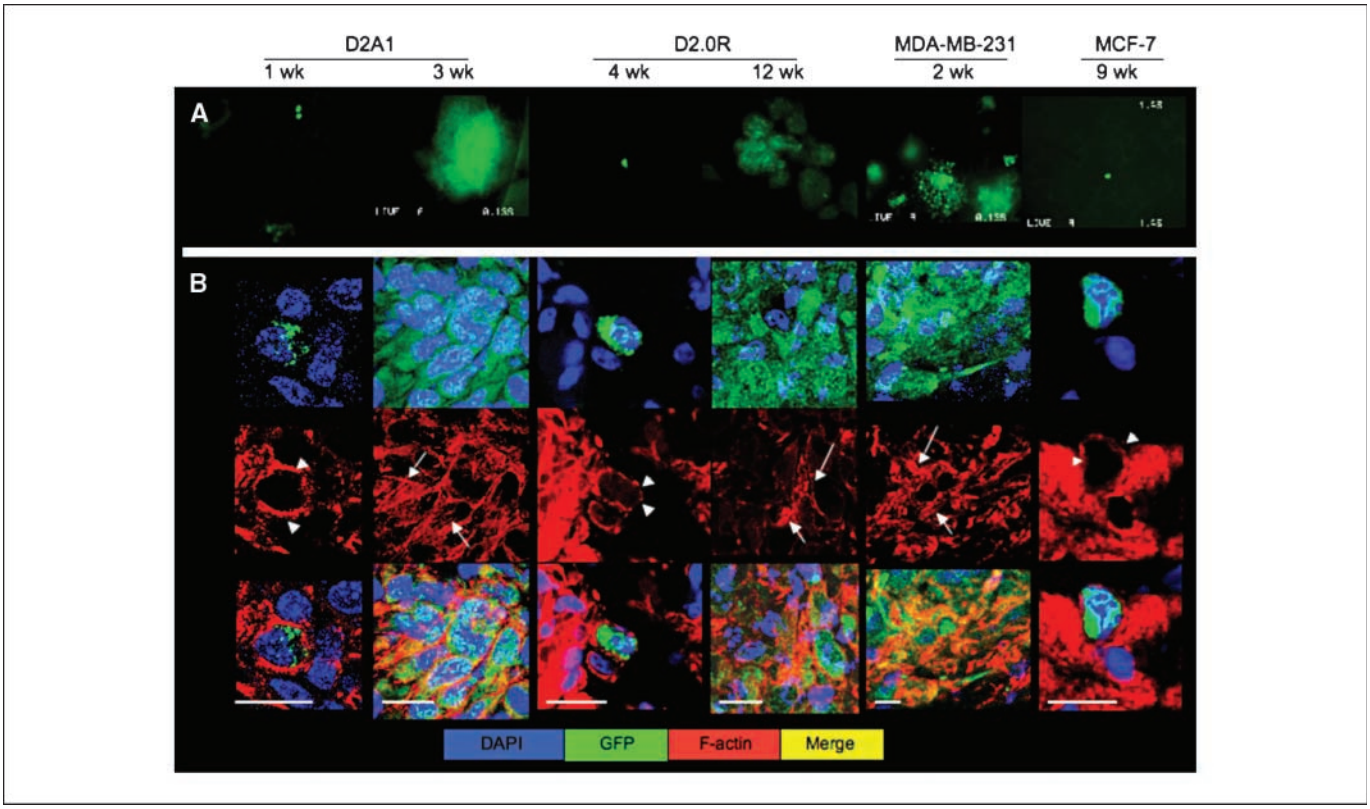

Figure 4. Cytoskeletal reorganization and formation of actin stress fibers during the switch from dormancy to metastatic growth. *A,* SCOM images (magnification, ×100) of lungs from mice injected with either D2A1-GFP (removed 1 or 3 wk after injection), D2.0R-GFP (removed 4 or 12 wk after injection), MDA-MB-231-GFP (removed 2 wk after injection), or MCF-7-GFP cells (removed 9 wk after injection). Time points varied according to the growth properties of the cells. *B,* frozen sections of lungs from mice injected with the above cells at the indicated time points stained for F-actin (*red*) using confocal microscopy. *Scale bar,* 20 μm. *White arrowheads,* cortical actin staining; *white arrows,* F-actin stress fibers.

D2.0R cells do not express fibronectin throughout the 14-day culture period in matrix (Fig. 6*A*). Importantly, both cell lines, as well as D2A1 metastatic lesions, express the fibronectin receptor integrin β1 (Fig. 6*A*; Supplementary Fig. S4*A*). However, expression of integrin β1 in D2.0R cells is reduced over time in the three-dimensional culture.

To functionally test whether fibronectin, through integrin β1, could induce the dormant-to-proliferative switch requiring activation of MLC, we blocked integrin β1 function through the addition of 150 μg/mL neutralizing antibody to integrin β1 to the overlay medium (see Materials and Methods). Inhibition of integrin β1 led to inhibition of MLC phosphorylation, loss of actin stress fiber formation, and significant inhibition of D2A1 proliferation (Fig. 6*B* and *D*; Supplementary Fig. S4*B*). Treatment with control IgG antibody had no effect. Supplementation of fibronectin to Cultrex (see Materials and Methods) induced spreading of D2A1 and D2.0R cells by day 3 (data not shown). By day 6, there was a greatly enhanced phosphorylation of MLC and actin stress fiber formation in both cell lines (Fig. 6*C*; Supplementary Fig. S5). Addition of fibronectin to the matrix also significantly enhanced cell proliferation of D2A1 cells by day 6 and led to a modest proliferation of D2.0R cells. However, fibronectin could not promote continuous proliferation of D2.0R cells by day 6 (Fig. 6*D*). The effect of fibronectin on both cell lines was significantly inhibited by the neutralizing antibody to integrin β1. Addition of ML-7 (5 μmol/L) at day 3 for 72 h inhibited the fibronectin effect on cell spreading and MLC phosphorylation in both cell lines but had a significant inhibitory effect on proliferation only on D2A1 cells (Fig. 6*C* and *D*; Supplementary Fig. S5). These results show that fibronectin signaling through integrin β1 activates phosphorylation of MLC by MLCK in D2A1 cells, leading to the transition from quiescence to growth.

Discussion

Mortality from breast cancer is primarily due to metastatic disease, which often appears years after successful treatment of the primary tumor, presumably due to the activation of latent, dormant metastatic tumor cells. Little is known about what maintains cellular dormancy and what evokes the emergence of proliferative metastatic growth from dormant tumor cells.

The focus of the present study has been to evaluate *in vitro* and *in vivo* models of solitary QTCs that precede the dormant micrometastatic stage and to show that growth of such cells can be highly influenced by the ECM. We report that quiescent or proliferative growth characteristics of tumor cells in a three-dimensional *in vitro* culture system can be correlated with their *in vivo* proliferative metastatic growth potential. This system provides a basis for exploring mechanisms involving the ECM that regulate the maintenance of cellular dormancy or the switch to proliferative metastatic growth.

Although all cells examined in this study readily proliferate in two-dimensional culture, an important finding of this work is the remarkably different growth characteristics of the cells in

three-dimensional culture that correlates with their proliferative characteristics as disseminated metastases to the lung. D2.0R, MCF-7, and K7M2AS1.46 cells, which remain dormant *in vivo*, are quiescent in three-dimensional culture, whereas highly metastatic D2A1, MDA-MB-231, and K7M2 cells readily proliferate in three-dimensional culture after variable but relatively short periods of quiescence. p16 and nuclear p27 were the predominant negative cell cycle regulators expressed in the quiescent cells, whereas their nuclear expression levels were significantly reduced in the cells that switched to a proliferative state.

There are several possibilities as to how the three-dimensional environment may influence quiescence or proliferation, including the presence or absence of growth factors, cytokines, proteases, or alterations in the composition or structure of ECM proteins. Previous reports have shown that contact with a component of the ECM inhibits metastatic melanoma cell proliferation (27, 28). Recent work has also shown that changes in tensile properties of the ECM may be important regulators of malignant transformation of tumor cells (29).

Striking differences in cell morphologies were observed between the quiescent and proliferative cells in three dimensional, leading us to explore further the cytoskeletal architecture of the cells in three dimensional because cell shape and cytoskeletal dynamics play critical roles in regulating cell cycle progression in anchorage-dependent cells by influencing molecular signaling pathways (6, 29–31). Results from our study suggest that the cytoskeletal configuration within the cell is a major regulator of the transition from cellular dormancy to a metastatic proliferative state. Significant morphologic differences are observed between the dormant and metastatic cell lines when placed in three-dimensional culture. The metastatic cells form actin stress fibers during their transition from quiescence to proliferation, which indicates a strong adherence of the cells to the ECM (32). In contrast, the quiescent cells remain rounded, with cortical actin staining, formation of filopodia representing transient attachment to the matrix, and no evidence of actin stress fiber formation *in vitro*.

A similar relationship between cytoskeletal dynamics and proliferative activity is observed when the cells are analyzed using an *in vivo* experimental metastasis model system. D2A1 and MDA-MB-231 cells undergo cytoskeletal reorganization with actin stress fiber formation during their transition from cellular dormancy to

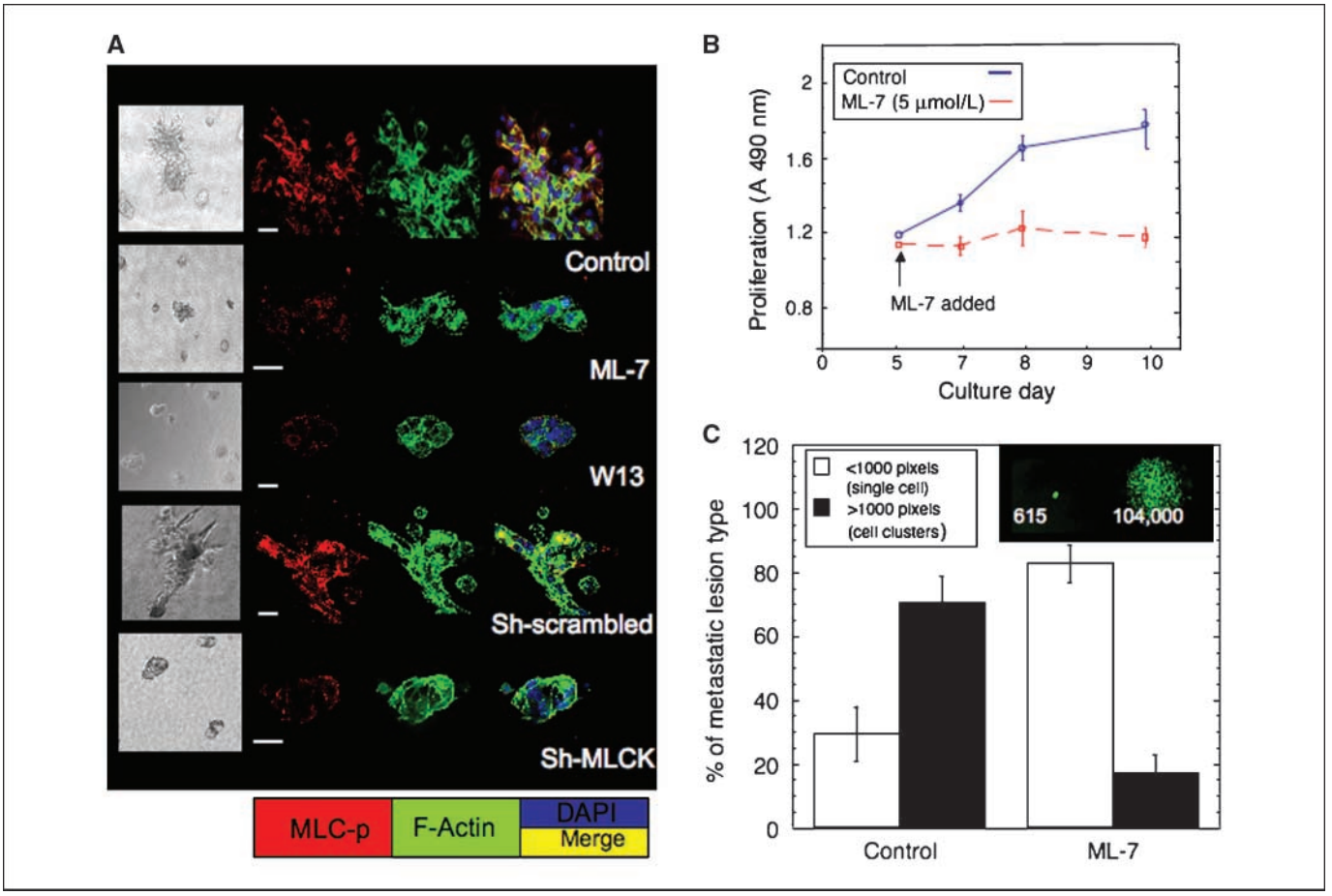

Figure 5. Inhibition of MLCK-mediated actin stress fiber formation blocks proliferation of metastatic cells in three-dimensional culture and reduces metastatic outgrowth in mice. *A,* D2A1 cells were cultured in three-dimensional Cultrex on glass coverslips. Cells were untreated (control) or treated with ML-7 (5 μmol/L) or W13 (5 μmol/L) for 48 h beginning on culture day 5 or treated with scrambled or MLCK shRNA as described in Materials and Methods and stained for the phosphorylated form of MLC (*red*), F-actin (*green*), and nuclei (*blue*). Merge of F-actin and phosphorylated MLC (*MLC-p*) staining (*yellow*) using light and confocal microscopy. Magnifications, ×40 and ×63, respectively. *Scale bars,* 20 μm. *B,* time course of D2A1 cell proliferation in three-dimensional Cultrex in the presence or absence of ML-7 (5 μmol/L). *Points,* mean ($n = 8$); *bars,* SE. *C,* inhibition of the metastatic outgrowth in lungs of mice treated with ML-7. Data presented as the percentage of single cells versus proliferative metastatic lesions in mice that received either ML-7 (22 mmol/L) or vehicle (control group; $P \leq 0.0001$ across all samples; $n = 9$). Single cells (<1,000 pixel intensity) and clusters of cells (>1,000 pixel intensity), as depicted in top right panel.

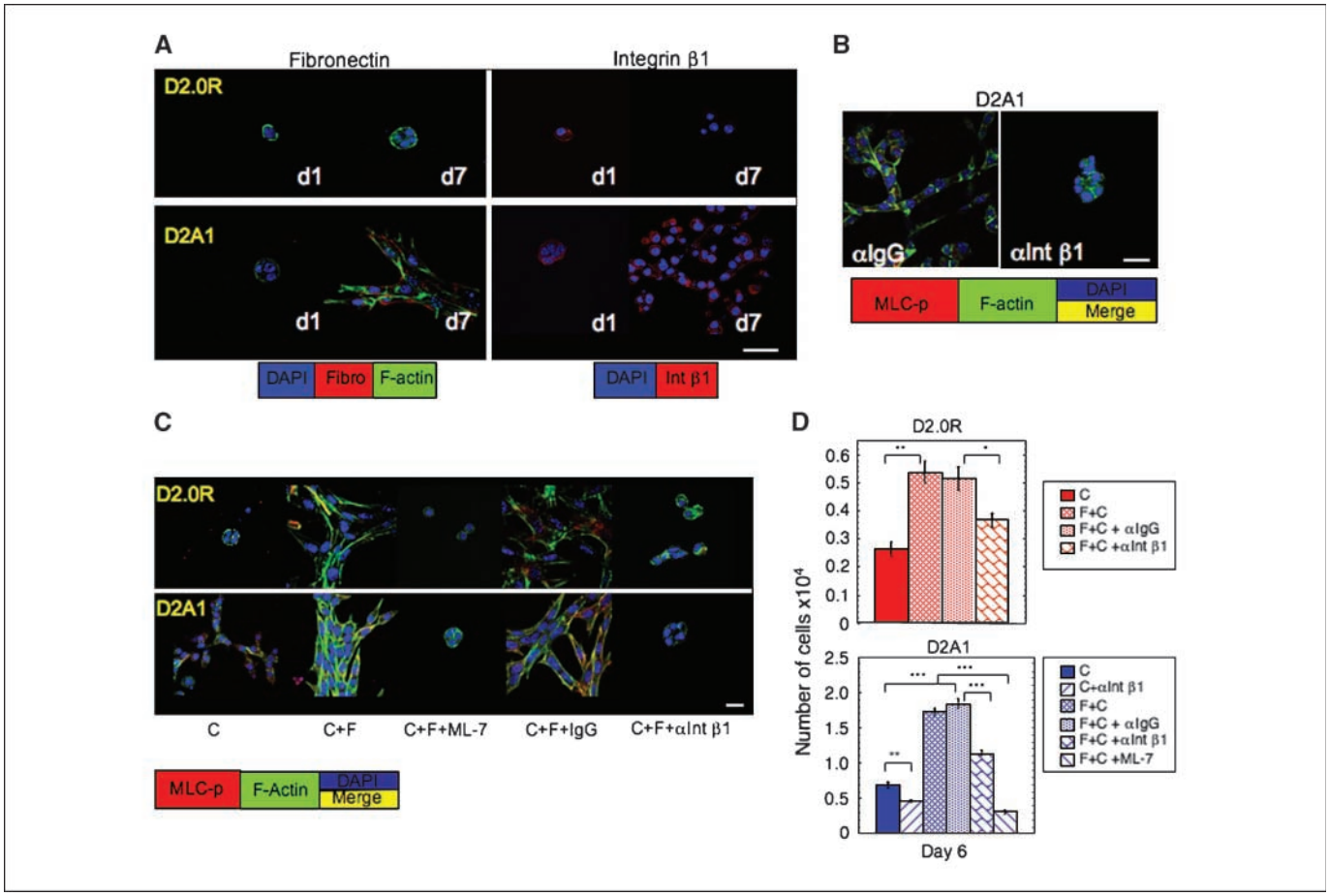

Figure 6. Fibronectin activates MLCK, leading to phosphorylation of MLC, actin stress fiber formation, and transition from quiescence to growth. D2.0R and D2A1 cells were cultured in three-dimensional Cultrex (*C*) on glass coverslips (as described in Materials and Methods). *A,* staining for fibronectin and integrin β1 (*Intβ1*) in D2.0R and D2A1 cells on days 1 and 7. *B* and *C,* D2A1 and D2.0R cells stained for phosphorylated MLC (*red*), F-actin (*green*), and nuclei (*blue*). *Yellow,* merge of F-actin and phosphorylated MLC staining. *B,* D2A1 cells treated with either control IgG or neutralizing antibody against integrin β1 for 6 d. *C,* D2.0R or D2A1 cells cultured on three-dimensional Cultrex mixed with fibronectin (*F+C*; 750 μg/mL) for 6 d in the presence of either nonspecific IgG (150 μg/mL), antibody against integrin β1 (150 μg/mL), or ML-7 (5 μmol/L) using confocal microscopy. Magnification, ×63. *Scale bar,* 20 μm.

proliferative metastases in the lung *in vivo*. Similarly, after a long latency, the occasional metastatic outgrows of D2.0R cells form actin stress fibers as well. MCF-7 cells do not form proliferative metastatic lesions in the lung but remain as solitary dormant cells with cortical actin staining.

To functionally assess the role of stress fiber formation in the dormant-to-proliferative switch, we attempted to inhibit actin stress fiber formation by blocking two known pathways involved in stress fiber formation: Rho kinase (32) and MLCK. Although Rho signaling is important in metastatic processes (33), inhibition of Rho did not inhibit stress fiber formation or the quiescent to proliferative switch of D2A1 cells in three-dimensional culture. However, inhibition of MLCK (either with shRNA, the inhibitor ML-7, or indirectly with W13 through inhibition of the MLCK activator calmodulin; ref. 34) prevented stress fiber formation and proliferative growth of D2A1, MDA-MB-231, and 4T1 cells in three-dimensional culture. This was accompanied by increased nuclear p27. Inhibition of proliferative outgrowth with W13 to block calmodulin function suggests that altering calcium flux may also significantly influence cytoskeletal dynamics and the dormant-to-proliferative switch of QTCs.

To determine whether inhibition of MLCK could reduce metastatic outgrowth *in vivo*, ML-7 or vehicle was given to mice whose lungs were seeded with D2A1 cells. A significant reduction in macrometastases and concomitant increase in single (dormant) cells was observed in mice receiving the MLCK inhibitor ML-7. These findings are consistent with a recent report that identified a direct correlation between levels of MLCK expression and reoccurrence of non–small cell lung cancer (35). Previous studies have shown that MLCK is involved in other key aspects of tumorigenesis, including the growth of primary tumors and tumor cell motility (36, 37). MLCK has also been localized in the cleavage furrow and may also play a role in this aspect of cell division and metastatic growth. This is the first demonstration that an inhibitor of MLCK and stress fiber formation can reduce metastases *in vivo* by apparently maintaining single cells in a quiescent state.

Given our demonstration that the ECM could greatly affect the proliferative characteristics of the metastatic cell lines we studied, and that ECM components have repeatedly been identified in metastatic signatures of various tumor types (25, 26), we sought to determine whether fibronectin, an ECM component often up-regulated in metastases (38) and present in the premetastatic niche (39), might be functionally involved in the transition of D2A1 cells from a quiescent to proliferative state. Fibronectin is not contained in the three-dimensional matrix we used.

Our results showed that proliferation of D2A1 cells was associated with fibronectin production, whereas the fibronectin receptor integrin β1 was continuously present in three-dimensional culture. D2.0R cells did not produce fibronectin in three-dimensional culture and integrin β1 expression diminished over time. Addition of fibronectin to the culture medium led to a modest proliferation of D2.0R cells and accelerated proliferation of D2A1 cells in three-dimensional culture with MLC phosphorylation and actin stress fiber formation. Importantly, we show that the proliferative outgrowth induced by fibronectin is mediated through integrin β1 and MLC phosphorylation, as either neutralizing antibody to integrin β1 or ML-7 inhibited proliferation. These results show that at least one component of the ECM, fibronectin, can regulate the proliferative outbreak of metastatic cells. However, fibronectin could not promote continuous proliferation of D2.0R cells. This may be a consequence of reduced integrin β1 expression in D2.0R cells or the failure of generating a self-sustained positive feedback loop that is needed to promote continuous growth (29, 40).

Additional factors are also likely necessary to initiate and sustain the dormant-to-proliferative switch. Future studies will address differences in the expression and activation of other integrins that interact with the ECM, which can lead to dramatic changes in the biological behavior of cells (29, 41–45). Additionally, interactions between the tumor cells and the ECM may induce proteolytic activities of metastatic cells that substantially alter the extracellular environment. Thus, differences in protease activities between dormant and metastatic cells may exist and can be explored in future studies.

Dormant metastatic tumor cells often evade standard adjuvant chemotherapies, which target actively proliferating cells (7). In this regard, the cellular dormancy may share biological features with cancer stem or progenitor cells. Our results suggest that targeting pathways affecting the cytoskeleton and, specifically, actin stress fiber formation may provide an important means of inhibiting the switch from tumor cell dormancy to clinical metastatic disease. This approach, perhaps in combination with immunotherapeutic strategies, may reduce the incidence of tumor recurrence from disseminated, dormant tumor cells.

Disclosure of Potential Conflicts of Interest

No potential conflicts of interest were disclosed.

Acknowledgments

Received 1/2/2008; revised 4/28/2008; accepted 5/13/2008.

Grant support: Intramural Research Program of the National Cancer Institute and National Dental Institute, NIH, and the Canadian Institutes of Health Research grant 42511. A.F. Chambers is Canada Research Chair in Oncology.

The costs of publication of this article were defrayed in part by the payment of page charges. This article must therefore be hereby marked *advertisement* in accordance with 18 U.S.C. Section 1734 solely to indicate this fact.

We thank Drs. Arnulfo Mendoza, Sung-Hyeok Hong, and Alexander N. Shoushtari for excellent technical support and Drs. Glenn Merlino, Stuart Yuspa, Kent Hunter, Judah Folkman, George Naumov, Mary Ann Stepp, and Primal de Lanerolle for useful discussions.

References

1. Pantel K, Schlimok G, Braun S, et al. Differential expression of proliferation-associated molecules in individual micrometastatic carcinoma cells. J Natl Cancer Inst 1993;85:1419–24.
2. Braun S, Vogl FD, Naume B, et al. A pooled analysis of bone marrow micrometastasis in breast cancer. N Engl J Med 2005;353:793–802.
3. Demicheli R. Tumour dormancy: findings and hypotheses from clinical research on breast cancer. Semin Cancer Biol 2001;11:297–306.
4. Goldberg SF, Harms JF, Quon K, Welch DR. Metastasis-suppressed C8161 melanoma cells arrest in lung but fail to proliferate. Clin Exp Metastasis 1999;17:601–7.
5. Naumov GN, MacDonald IC, Weinmeister PM, et al. Persistence of solitary mammary carcinoma cells in a secondary site: a possible contributor to dormancy. Cancer Res 2002;62:2162–8.
6. Aguirre-Ghiso JA. Models, mechanisms and clinical evidence for cancer dormancy. Nat Rev Cancer 2007;7:834–46.
7. Naumov GN, Townson JL, MacDonald IC, et al. Ineffectiveness of doxorubicin treatment on solitary dormant mammary carcinoma cells or late-developing metastases. Breast Cancer Res Treat 2003;82:199–206.
8. Naumov GN, Bender E, Zurakowski D, et al. A model of human tumor dormancy: an angiogenic switch from the nonangiogenic phenotype. J Natl Cancer Inst 2006;98:316–25.
9. Fidler IJ. The organ microenvironment and cancer metastasis. Differentiation 2002;70:498–505.
10. Bissell MJ, Radisky DC, Rizki A, Weaver VM, Petersen OW. The organizing principle: microenvironmental influences in the normal and malignant breast. Differentiation 2002;70:537–46.
11. Gassmann P, Enns A, Haier J. Role of tumor cell adhesion and migration in organ-specific metastasis formation. Onkologie 2004;27:577–82.
12. Nelson CM, Bissell MJ. Modeling dynamic reciprocity: engineering three-dimensional culture models of breast architecture, function, and neoplastic transformation. Semin Cancer Biol 2005;15:342–52.
13. Shaw KR, Wrobel CN, Brugge JS. Use of three-dimensional basement membrane cultures to model oncogene-induced changes in mammary epithelial morphogenesis. J Mammary Gland Biol Neoplasia 2004;9:297–310.
14. Morris VL, Koop S, MacDonald IC, et al. Mammary carcinoma cell lines of high and low metastatic potential differ not in extravasation but in subsequent migration and growth. Clin Exp Metastasis 1994;12:357–67.
15. Aslakson CJ, Miller FR. Selective events in the metastatic process defined by analysis of the sequential dissemination of subpopulations of a mouse mammary tumor. Cancer Res 1992;52:1399–405.
16. Khanna C, Wan X, Bose S, et al. The membrane-cytoskeleton linker ezrin is necessary for osteosarcoma metastasis. Nat Med 2004;10:182–6.
17. Harms JF, Budgeon LR, Christensen ND, Welch DR. Maintaining GFP tissue fluorescence through bone decalcification and long-term storage. Biotechniques 2002;33:1197–200.
18. Debnath J, Muthuswamy SK, Brugge JS. Morphogenesis and oncogenesis of MCF-10A mammary epithelial acini grown in three-dimensional basement membrane cultures. Methods 2003;30:256–68.
19. Ventura A, Meissner A, Dillon CP, et al. Cre-lox-regulated conditional RNA interference from transgenes. Proc Natl Acad Sci U S A 2004;101:10380–5.
20. Morris VL, Tuck AB, Wilson SM, Percy D, Chambers AF. Tumor progression and metastasis in murine D2 hyperplastic alveolar nodule mammary tumor cell lines. Clin Exp Metastasis 1993;11:103–12.
21. Thompson EW, Brunner N, Torri J, et al. The invasive and metastatic properties of hormone-independent but hormone-responsive variants of MCF-7 human breast cancer cells. Clin Exp Metastasis 1993;11:15–26.
22. Klemke RL, Cai S, Giannini AL, Gallagher PJ, de Lanerolle P, Cheresh DA. Regulation of cell motility by mitogen-activated protein kinase. J Cell Biol 1997;137:481–92.
23. Saitoh M, Ishikawa T, Matsushima S, Naka M, Hidaka H. Selective inhibition of catalytic activity of smooth muscle myosin light chain kinase. J Biol Chem 1987;262:7796–801.
24. Nairn AC, Picciotto MR. Calcium/calmodulin-dependent protein kinases. Semin Cancer Biol 1994;5:295–303.
25. Ramaswamy S, Ross KN, Lander ES, Golub TR. A molecular signature of metastasis in primary solid tumors. Nat Genet 2003;33:49–54.
26. Qiu TH, Chandramouli GV, Hunter KW, Alkharouf NW, Green JE, Liu ET. Global expression profiling identifies signatures of tumor virulence in MMTV-PyMT-transgenic mice: correlation to human disease. Cancer Res 2004;64:5973–81.
27. Henriet P, Zhong ZD, Brooks PC, Weinberg KI, DeClerck YA. Contact with fibrillar collagen inhibits melanoma cell proliferation by up-regulating p27KIP1. Proc Natl Acad Sci U S A 2000;97:10026–31.
28. Roth JM, Akalu A, Zelmanovich A, et al. Recombinant α2(IV)NC1 domain inhibits tumor cell-extracellular matrix interactions, induces cellular senescence, and inhibits tumor growth *in vivo*. Am J Pathol 2005;166:901–11.
29. Paszek MJ, Zahir N, Johnson KR, et al. Tensional homeostasis and the malignant phenotype. Cancer Cell 2005;8:241–54.
30. Huang S, Ingber DE. Shape-dependent control of cell growth, differentiation, and apoptosis: switching between attractors in cell regulatory networks. Exp Cell Res 2000;261:91–103.
31. Folkman J, Moscona A. Role of cell shape in growth control. Nature 1978;273:345–9.
32. Defilippi P, Olivo C, Venturino M, Dolce L, Silengo L, Tarone G. Actin cytoskeleton organization in response to integrin-mediated adhesion. Microsc Res Tech 1999;47:67–78.
33. Tang Y, Olufemi L, Wang MT, Nie D. Role of Rho GTPases in breast cancer. Front Biosci 2008;13:759–76.
34. Somlyo AP, Somlyo AV. Signal transduction and regulation in smooth muscle. Nature 1994;372:231–6.

35. Minamiya Y, Nakagawa T, Saito H, et al. Increased expression of myosin light chain kinase mRNA is related to metastasis in non-small cell lung cancer. Tumour Biol 2005;26:153–7.
36. Kaneko K, Satoh K, Masamune A, Satoh A, Shimosegawa T. Myosin light chain kinase inhibitors can block invasion and adhesion of human pancreatic cancer cell lines. Pancreas 2002;24:34–41.
37. Fazal F, Gu L, Ihnatovych I, et al. Inhibiting myosin light chain kinase induces apoptosis *in vitro* and *in vivo*. Mol Cell Biol 2005;25:6259–66.
38. Feng Y, Sun B, Li X, et al. Differentially expressed genes between primary cancer and paired lymph node metastases predict clinical outcome of node-positive breast cancer patients. Breast Cancer Res Treat 2007; 103:319–29.
39. Kaplan RN, Rafii S, Lyden D. Preparing the "soil": the premetastatic niche. Cancer Res 2006;66:11089–93.
40. Larsen M, Artym VV, Green JA, Yamada KM. The matrix reorganized: extracellular matrix remodeling and integrin signaling. Curr Opin Cell Biol 2006;18: 463–71.
41. Weaver VM, Petersen OW, Wang F, et al. Reversion of the malignant phenotype of human breast cells in three-dimensional culture and *in vivo* by integrin blocking antibodies. J Cell Biol 1997;137:231–45.
42. Aguirre Ghiso JA, Kovalski K, Ossowski L. Tumor dormancy induced by downregulation of urokinase receptor in human carcinoma involves integrin and MAPK signaling. J Cell Biol 1999;147:89–104.
43. Korah R, Boots M, Wieder R. Integrin $\alpha5\beta1$ promotes survival of growth-arrested breast cancer cells: an *in vitro* paradigm for breast cancer dormancy in bone marrow. Cancer Res 2004;64:4514–22.
44. Walker JL, Fournier AK, Assoian RK. Regulation of growth factor signaling and cell cycle progression by cell adhesion and adhesion-dependent changes in cellular tension. Cytokine Growth Factor Rev 2005;16:395–405.
45. White DE, Kurpios NA, Zuo D, et al. Targeted disruption of $\beta1$-integrin in a transgenic mouse model of human breast cancer reveals an essential role in mammary tumor induction. Cancer Cell 2004;6:159–70.